Journal of Physics: Conference Series **3177** (2026) 012120 doi:10.1088/1742-6596/3177/1/012120

Narrowband search for continuous gravitational waves from known pulsars using O4 LVK data

Lorenzo Mirasola[1,2] on behalf of the LIGO, Virgo and KAGRA Collaborations

[1]Physics Department, Università degli Studi di Cagliari, Cagliari 09042, Italy
[2]INFN, Sezione di Cagliari, Cagliari 09042, Italy

E-mail: lorenzo.mirasola@ligo.org

Abstract. We present a summary of the narrowband search for continuous gravitational waves (CWs) emitted by a set of 16 known pulsars using data from the first part of the fourth LIGO–Virgo–KAGRA observing run, known as O4a. We searched for a CW emission not strictly locked to the electromagnetic emission, without finding any evidence for such signals in O4a data. Therefore, we set upper limits on the signal amplitude emitted by each target.

1 Introduction

This contribution summarises an analysis previously published in [1].

Rotating neutron stars, non-symmetric with respect to their rotation axis, are eligible and potentially detectable sources for continuous gravitational waves (CWs) [2]. CWs are long-lasting gravitational-wave signals with amplitude and frequency exhibiting small variations over year-long timescales. Possible mechanisms of CW emission from neutron stars are discussed in greater detail in [2, 3].

Since their discovery in 1967, pulsars have played a crucial role in advancing our understanding of fundamental physics. These extremely dense and compact objects possess strong magnetic fields and rotate rapidly, emitting beams of electromagnetic (EM) radiation from hot spots near the poles or from the higher magnetosphere [4].

One of the main challenges for CW search lies in accurately accounting for the various modulations that affect the signal received at the detector. These include the Doppler effect due to the Earth's motion, the CW frequency evolution (i.e., the secular spin-down $\dot{f}$) and relativistic effects. Pulsar's EM observations provide accurate measurements of the sky position and rotation parameters, allowing us to predict and correct these modulations, thereby enhancing the search sensitivity.

Depending on the accuracy with which parameters are known, the optimal CW search strategy may vary [5]. *Narrowband searches* aim to detect CWs from known pulsars at twice their rotational frequency, $2f_{\rm rot}$, using full-coherent methods that integrate data over long observation times, maintaining phase coherence over time. By assuming that the GW phase evolution follows closely the EM solution, the search explores a narrow band around the measured frequency and spin-down rate (e.g., [6, 7, 8, 1, 9]). However, because these searches are not computationally cheap, they are often performed on a few interesting targets for which we expect a (potentially) detectable CW emission.

A scenario where GW and EM emissions have similar, but slightly different phase evolution is plausible, e.g., when there is differential rotation between the rigid crust and superfluid parts of the star. Possible observational evidence for this comes, for example, from pulsar glitches [10, 11]. In many models [12], the superfluid and non-superfluid components build up a lag with respect to one another, with the glitch representing the sudden re-coupling of the two [13, 14].

2 Signal model

The narrowband search performed in [1] makes use of the *5-vector* formalism introduced in [15, 16]. We expect the CW signal to be described by the real part of

$$h(t) = H_0 \left(H_+ \mathbf{A}^+ + H_\times \mathbf{A}^\times\right) \cdot \mathbf{W}\, e^{j\phi(t))}, \tag{1}$$

where $\phi(t)$ encloses the spin-down and Doppler modulation effects, and boldface symbols denote 5-vectors (arrays with five complex components). The vectors $\mathbf{A}^{+/\times}$ represent detector response templates to the two GW polarizations, and $\mathbf{W} = e^{jk\Theta}$ encodes sidereal modulation, with $k = \{0, \pm 1, \pm 2\}$ and Θ the local sidereal angle. On the other hand, the CW polarisations are expressed as

$$H_+ = \frac{\cos(2\psi) - j\eta\sin(2\psi)}{\sqrt{1+\eta^2}}, \qquad H_\times = \frac{\sin(2\psi) + j\eta\cos(2\psi)}{\sqrt{1+\eta^2}}, \tag{2}$$

with η and ψ polarisation parameters, and H_0 is related to the standard gravitational wave amplitude h_0 as $H_0 = h_0/2 \cdot \sqrt{1 + 6\cos^2\iota + \cos^4\iota}$.

After accounting for Doppler modulation and spin-down effects, see [16], the signal power is spread over five harmonics due to the detector's response to a CW. The central peak, at the CW frequency $f_{\rm gw}$, has four sidebands whose distance to the central peak is $\pm 1, \pm 2 f_\oplus$ where $f_\oplus$ is the Earth's sidereal rotation frequency. For an isolated triaxial star, rotating steadily about one of its principal axes of inertia, the GW emission frequency is twice the pulsar's spin frequency, $f_{\rm rot}$ [2, 5].

We search for a CW by making use of the matched filters $\hat{H}_{+/\times}$ computed in the frequency domain as

$$\hat{H}_{+/\times} = \frac{\mathbf{X} \cdot \mathbf{A}^{+/\times}}{|\mathbf{A}^{+/\times}|^2}, \tag{3}$$

where $\mathbf{X}$ is the data 5-vector composed of the Fourier power at the five harmonics of interest. Our detection statistic is defined as [15, 17, 18]

$$\mathcal{S} = |\mathbf{A}^+|^4 |\hat{H}_+|^2 + |\mathbf{A}^\times|^4 |\hat{H}_\times|^2\,, \tag{4}$$

extendable to a multi-detector analysis following [16, 19]. This formulation enables the efficient estimation of signal amplitudes within a maximum likelihood framework and offers improved sensitivity when the signal has unequal contributions from the two polarisations [15].

3 Search setup

The 5n-vector narrowband pipeline has been described in [20, 18] and explores a narrow frequency and spin-down range around twice the ephemeris observations, namely

$$f \in 2 f_{\rm rot}[1-\delta,\, 1+\delta]\,, \tag{5}$$

usually $\delta = 10^{-3}$ [8, 1], and a similar equation for $\dot{f}$. We build the template grid by considering all the resolved parameter-space points within the region of interest. The grid spacing is calculated using the resolution calculated as [20] $\delta f = 1/T_{\rm obs}$, and $\delta \dot{f} = 1/T_{\rm obs}^2$, with $T_{\rm obs}$, the data timespan. Higher-order spin-down terms, if provided in the ephemerides, are fixed at twice the rotation terms to track the GW frequency evolution over time, without exploring any additional template [17]. After a frequency-independent Doppler correction, we evaluate Equation (4) for each explored template. From the collection of $\mathcal{S}$ values, we order them along the frequency axis to select the maximum every 10^{-4} Hz, marginalising over the spin-down. We use a p-value threshold (i.e., the tail probability of the noise-only distribution) of 1% after accounting for the trial factor to determine whether a point is statistically significant. The noise-only distribution is inferred from the tail of the histogrammed non-maxima values, which is fitted with an exponential [21].

If CW detection is not claimed, we set the 95% confidence level (CL) upper limit $h_0^{95\%}$ through software-injection campaigns.

4 Target selection and search results

The sensitivity of the search depends on the number of explored templates [17, 22], the effective $T_{\rm obs}$ (i.e., corrected for the duty cycle) and its noise level expressed by the unilateral noise power spectral density (PSD). In [1], we analyse those targets with spin-down limit $h_0^{\rm sd}$ above the estimated sensitivity. This

limit is the maximum GW amplitude allowed, assuming all the lost rotational energy of the star is due to conversion into GW energy.

We consider data from the first part of the fourth observing run, known as O4a, of the LIGO Livingston (L1) and LIGO Hanford (H1) detectors [23]. See [24] for more details on O4a data quality. As a result, we select 16 isolated[1] targets out of which 8 have not been analysed in [8]. Our dataset includes two glitching pulsars for which we split O4a data into two segments that exclude from the analysis the period around [t_g-1 d, t_g+2 d], with t_g the glitch epoch. The segments are then analysed independently. See Figure 1 of [1] for the target's sky location.

We report no statistically-significant outliers, with a p-value below 10^{-2} after accounting for the trial factor, for none of the targets. In the absence of any detections, we have calculated upper limits at the 95% CL for each of the analysed targets. Our results are listed in Table 3 of [1] and shown in Figure 1 comparing them with the expected sensitivity.

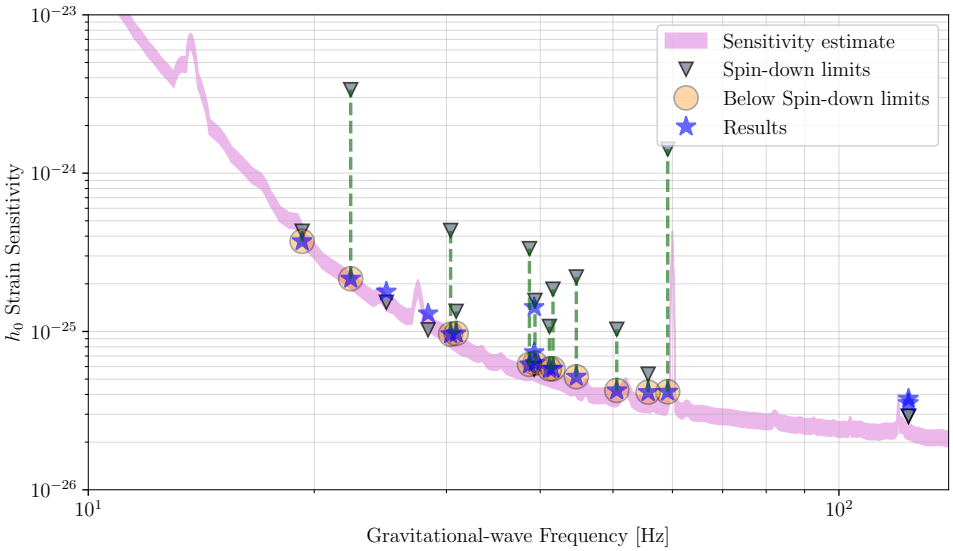

Figure 1: Expected sensitivity of the narrowband search using O4a (shaded pink region) dataset from the two LIGO detectors. The curve is compared with the spin-down limits (triangles) and the upper limits (stars) averaged over all the 10^{-4} Hz bands for each source. Upper limits below the spin-down limit are highlighted with orange circles. Reproduced from [1].

Out of the 16 analysed targets, 12 searches report an upper limit below the corresponding spin-down limit (see Tab. 3 of [1]), ranging from a factor of 1.16 for J2021+3651 to 33 for J0534+2200. The targets analysed with O3 data [8] report upper limits comparable to those in Fig 1. This is readily explained by a general improvement of O4a PSDs by almost a factor of 1.5 to 2 compared to the corresponding O3 ones, depending on the considered frequency band. On the other hand, the effective observation time for O4a is reduced by a factor of approximately 1.6, which diminishes the benefit of the improved detector sensitivity in O4a.

5 Conclusions

In this work, we present a search for CW signals from a set of 16 known pulsars using O4a data from the two LIGO detectors using the 5n-vector narrowband pipeline. Pulsars are chosen considering an expected sensitivity for the amplitude below the theoretical spin-down limit. EM observations were employed to constrain the pulsars' sky positions and rotational parameters covering the O4a data period. For 12 targets, we report an upper limit below the spin-down one, constraining the fraction of emitted energy through the CW channel.

Analyses of the entire O4 dataset will set more stringent constraints thanks to the longest-ever observing run and new detector upgrades.

[1]The current version of the pipeline does not account for an additional orbital modulation if the source is in a binary system.

Acknowledgements
Acknowledgements may be found in `https://dcc.ligo.org/P2100218/public`

References

[1] Abac A G *et al.* (LIGO Scientific, VIRGO, KAGRA) 2025 *Astrophys. J.* **983** 99 (*Preprint* 2501.01495)

[2] Riles K 2023 *Living Rev. Rel.* **26** 3 (*Preprint* 2206.06447)

[3] Glampedakis K and Gualtieri L 2018 *Gravitational Waves from Single Neutron Stars: An Advanced Detector Era Survey* vol 457 p 673

[4] Philippov A and Kramer M 2022 *Annual Review of Astronomy and Astrophysics* **60** 495–558 ISSN 1545-4282 URL https://www.annualreviews.org/content/journals/10.1146/annurev-astro-052920-112338

[5] Wette K 2023 *Astropart. Phys.* **153** 102880 (*Preprint* 2305.07106)

[6] Abbott B P *et al.* (LIGO Scientific, Virgo) 2017 *Phys. Rev. D* **96** 122006 [Erratum: Phys.Rev.D 97, 129903 (2018)] (*Preprint* 1710.02327)

[7] Abbott B P *et al.* (LIGO Scientific, Virgo) 2019 *Phys. Rev. D* **99** 122002 (*Preprint* 1902.08442)

[8] Abbott R *et al.* (LIGO Scientific, KAGRA, VIRGO) 2022 *Astrophys. J.* **932** 133 (*Preprint* 2112.10990)

[9] Ashok A, Beheshtipour B, Papa M A, Freire P C C, Steltner B, Machenschalk B, Behnke O, Allen B and Prix R 2021 *Astrophys. J.* **923** 85 (*Preprint* 2107.09727)

[10] Espinoza C M, Lyne A G, Stappers B W and Kramer M 2011 *MNRAS* **414** 1679–1704 ISSN 0035-8711 (*Preprint* 1102.1743)

[11] Haskell B 2017 *IAU Symp.* **337** 203–208 (*Preprint* 1712.01547)

[12] Haskell B and Melatos A 2015 *Int. J. Mod. Phys. D* **24** 1530008 (*Preprint* 1502.07062)

[13] Anderson P W and Itoh N 1975 *Nature* **256** 25–27

[14] Lyne A G, Shemar S L and Smith F G 2000 *Mon. Not. Roy. Astron. Soc.* **315** 534–542

[15] Astone P, D'Antonio S, Frasca S and Palomba C 2010 *CQGra* **27** 194016

[16] Astone P, Colla A, D'Antonio S, Frasca S and Palomba C 2012 *J. Phys. Conf. Ser.* **363** 012038 (*Preprint* 1203.6733)

[17] Astone P, Colla A, D'Antonio S, Frasca S, Palomba C and Serafinelli R 2014 *Phys. Rev. D* **89** 062008 (*Preprint* 1403.1484)

[18] Mastrogiovanni S, Astone P, D'Antonio S, Frasca S, Intini G, Leaci P, Miller A, Palomba C, Piccinni O J and Singhal A 2017 *Class. Quant. Grav.* **34** 135007 (*Preprint* 1703.03493)

[19] D'Onofrio L, De Rosa R and Palomba C 2024 A weighted multidetector extension to the 5-vector method for the search of continuous gravitational wave signals *Proceedings of XVIII International Conference on Topics in Astroparticle and Underground Physics — PoS(TAUP2023)* vol 441 p 109

[20] Astone P, Colla A, D'Antonio S, Frasca S, Palomba C and Serafinelli R 2014 *Phys. Rev. D* **89**(6) 062008 URL https://link.aps.org/doi/10.1103/PhysRevD.89.062008

[21] Singhal A, Leaci P, Astone P, D'Antonio S, Frasca S, Intini G, Rosa I L, Mastrogiovanni S, Miller A, Muciaccia F, Palomba C and Piccinni O 2019 *Classical and Quantum Gravity* **36** 205015 URL https://dx.doi.org/10.1088/1361-6382/ab4367

[22] D'Onofrio L, Astone P, Pra S D, D'Antonio S, Giovanni M D, Rosa R D, Leaci P, Mastrogiovanni S, Mirasola L, Muciaccia F, Palomba C and Pierini L 2024 *Classical and Quantum Gravity* **42** 015005 URL https://dx.doi.org/10.1088/1361-6382/ad94c5

[23] Aasi J *et al.* (LIGO Scientific) 2015 *Class. Quant. Grav.* **32** 074001 (*Preprint* 1411.4547)

[24] Soni S *et al.* 2024 Ligo detector characterization in the first half of the fourth observing run (*Preprint* 2409.02831) URL https://arxiv.org/abs/2409.02831